Novel ZnFe$_2$O$_4$/TiO$_2$/flake graphite composite as particle electrodes for efficient photoelectrocatalytic degradation of rhodamine B in water

Dan Jia, Jian Yu, Stephen M. Long and Hao L. Tang

ABSTRACT

A novel ZnFe$_2$O$_4$/TiO$_2$/flake graphite composite material was synthesized and used as particle electrodes in a photoelectrocatalytic (PEC) system to investigate the degradation of rhodamine B as a model dye pollutant in water. Results showed that a PEC process with the new composite evidently led to enhanced degradation of rhodamine B due to a synergistic effect of photocatalysis and electrocatalysis. Operating variables including electrolyte concentration, applied cell voltage, air flow, composite dosage, solution pH, and dye concentration were also found to play important roles in rhodamine B removal. A 99.0% removal efficiency was observed within 30 min of treatment under optimum conditions of 0.01 mol/L Na$_2$SO$_4$, applied cell voltage of 15 V, air flow of 20 mL/min, composite dosage of 10 g/L, solution pH of 2, and rhodamine B concentration of 20 mg/L, with a pseudo-first-order rate constant of 0.278 min^{-1}. These findings could provide new insights into the development of efficient PEC technologies on degradation of residual dyes in water.

Key words | flake graphite, particle electrode, photoelectrocatalysis, titanium oxide, zinc ferrite

Dan Jia
Jian Yu (corresponding author)
Department of Water Engineering and Science,
  College of Civil Engineering,
Hunan University,
Changsha, Hunan 410082,
China
E-mail: *jianyu@hnu.edu.cn*

Stephen M. Long
Hao L. Tang
Department of Chemistry,
Indiana University of Pennsylvania,
Indiana, Pennsylvania 15705,
USA

INTRODUCTION

In recent years, dyes have been frequently used in textile industries and the untreated dyes are often discharged into natural streams, causing a growing environmental concern about contamination of drinking water (Mourão *et al.* 2010). Most dyes are potentially carcinogenic and resist biological methods to decompose (Liu *et al.* 2012) due to their large and complex molecular structures, posing a great challenge for color removal and complete mineralization. Advanced oxidation technologies (AOTs) that can generate highly powerful free radicals such as hydroxyl radicals (•OH) have been found useful in the degradation of most dyes. Among them, photocatalytic oxidation represents a promising AOT in the degradation of dyes due to its low cost, formation of less harmful secondary byproducts, operability under standard atmospheric condition, and utilization of renewable solar energy (Lee *et al.* 2013).

The AOT based on the heterogeneous semiconductor has reactions occurring at the surface of photocatalysts. However, the recombination of photoinduced electron-hole pairs at the surface is an inevitable issue. In addition, powdered photocatalysts are difficult to separate and recycle

from the reaction system. Therefore, effective approaches for restraining electron-hole pair recombination and recycling photocatalysts are highly desirable. To solve the first limitation, a photoelectrocatalytic (PEC) process that uses an external electric circuit has been proposed by combining the photocatalytic and electrocatalytic technologies. A PEC reactor has an applied external anodic bias, which drives the photoinduced electrons and holes in different directions to effectively restrict the photoinduced electron-hole pair recombination (Zhai *et al.* 2013). The second limitation on separation and recovery of the suspended photocatalysts can be solved by immobilization of semiconductors onto the electrodes using a two-dimensional or a three-dimensional electrode system (Liu *et al.* 2012; Ayoubi-Feiz *et al.* 2014). An *et al.* (2002) investigated the PEC degradation of methylene blue with a three-dimensional electrode system and found 95% decolorization efficiency and 87% COD reduction were achievable. Since the titanium dioxide (TiO$_2$) photocatalysts they used were in a powdered form, their further research (An *et al.* 2004) on degradation of quinoline used TiO$_2$ aggregated sand as particle electrodes for

easy separation and recovery. However, the packed bed sand in a compact reactor may affect the light transmittance, and the weight percentage of the semiconductor in the sand aggregate is low due to limited active sites in the sand structure, which potentially inhibit the PEC degradation efficiency. A better support medium for efficient PEC degradation of dyes is needed.

To date, little information has been available on using flake graphite as a support medium for heterogeneous semiconductor aggregation. As a carbonaceous material, flake graphite has more active sites for aggregation of semiconductors compared to the conventional sand media. The adsorption of dye pollutants to the surface also allows for easy oxidation by the produced ·OH. In addition, the crystallinity feature of flake graphite leads to efficient photocatalytic activity (Pan *et al.* 2010), and its good conductivity contributes to easy polarization by external electric field for the formation of numerous charged microelectrodes. Therefore, it would be meaningful to investigate the potential of using flake graphite as particle electrodes in a three-dimensional PEC system. Specifically, it is speculated that the incorporation of zinc ferrite ($ZnFe_2O_4$) into the TiO_2 structure might benefit the photocatalytic performance due to a relatively narrow band-gap (ca. 1.9 eV), because the band overlap could promote the excitation of the valence band electrons. Besides, the use of microelectrodes shortens the distance between the reactants and the electrodes, increases the surface area of the electrode and mass transfer, and thus might benefit the electrocatalytic performance. Thus, a synergistic effect of a visible-light-responsive photocatalyst, a new support medium, and a three-dimensional PEC system design is worth investigating.

In this work, we demonstrate a novel $ZnFe_2O_4/TiO_2/$ flake graphite composite material as particle electrodes in a three-dimensional electrode system for the PEC degradation of rhodamine B as a model dye pollutant. Rhodamine B, a widely used fluorescent dye, has been linked with potential toxicity, mutagenicity and carcinogenic effects, and is an important representative xanthene dye with good stability and high water solubility. The objectives of this research are two-fold: (1) to prepare a $ZnFe_2O_4/TiO_2/$flake graphite composite material by immobilizing $ZnFe_2O_4$ and TiO_2 on flake graphite using a sol-gel method; (2) to investigate the PEC performance with the composite for rhodamine B removal under various operating conditions. The research could provide new insights into the development of efficient PEC technologies on degradation of residual dyes in water.

MATERIALS AND METHODS

Materials

All reagents and chemicals used were of analytical grade without further purification. Tetrabutyl titanate (Tianjin Kemiou Chemical Reagent Co. Ltd, China), zinc acetate (Shanghai Shanpu Chemical Co. Ltd, China) and ferric nitrate (Xilong Chemical Co. Ltd, China) were used as the sources for Ti, Zn and Fe respectively. Rhodamine B (Tianjin Guangfu Fine Chemical Research Institute, China) was used as the model dye pollutant for the degradation study.

Composite preparation

Flake graphite with a diameter range between 0.38 and 0.83 mm was pre-washed with distilled water to remove any impurities and dried at 110 °C. The composite was prepared by a sol-gel process as follows: Solution A was made by dissolving 10 mL tetrabutyl titanate in 20 mL anhydrous ethanol, followed by adding 6 mL glacial acetic acid and stirring for 1 h. Solution B was prepared by mixing zinc acetate and ferric nitrate based on a Zn:Fe molar ratio of 1:2 with 20 mL anhydrous ethanol, followed by adding 3 mL distilled water and stirring for 1 h. Solution B was added dropwise to solution A at 1 drop per second while stirring to form a yellow gel. Ten grams of flake graphite were added to the yellow gel, stirred for 1 h, and sealed at room temperature for 24 h. Filtration was then applied to remove extra gel that did not attach to the flake graphite, and the residue was dried at 110 °C and calcined for 2 h in a muffle furnace at 450 °C. The formed composite was stored in a desiccator after ambient air cooling.

Characterization

The surface morphology and structure of the $ZnFe_2O_4/TiO_2/$flake grahite composite was characterized by N_2 physisorption using the Brunauer-Emmett-Teller (BET) isotherm, scanning electron microscopy (SEM, Hitachi Model S-4800, Hitachi High-Technologies Corporation, Japan), X-ray diffraction (XRD, M21X, MAC Science Ltd, Japan) using Cu Kα radiation, and X-ray photoelectron spectroscopy (XPS, K-Alpha 1063, Thermo Fisher Scientific Inc., UK).

PEC reactor

The PEC system (Figure 1) was composed of a quartz reactor with a capacity of 250 mL, a magnetic stirrer, a
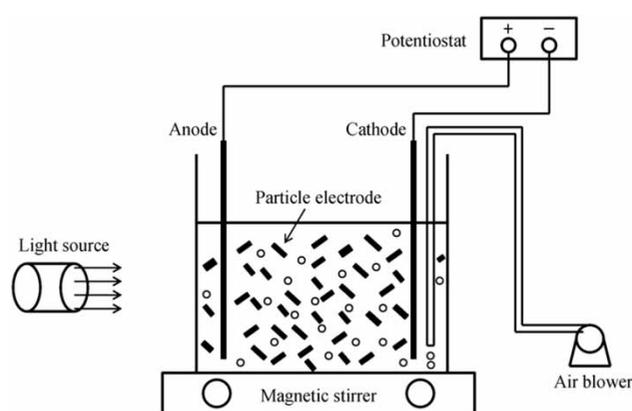
Figure 1 │ Schematic diagram of the PEC system.

potentiostat, diffused air, a light source at the side of the reactor, two Pt plates (10 cm × 4.5 cm, effective area 4.0 cm × 4.5 cm) as anode and cathode, and the prepared $ZnFe_2O_4/TiO_2$/flake graphite composite as particle electrodes. The reactor contained 100 mL rhodamine B solution as target dye pollutant and Na_2SO_4 as electrolyte. The distance between the light source and the reactor was 25 cm. The two Pt plates were divided by securing to the opposing side walls of the reactor.

Degradation studies and analysis

A 500 W xenon lamp (CHF-XM-500 W, Beijing Zhongxing Weiye Instrument Co. Ltd, China) was used for illumination, which emitted both UV and visible light over a wide wavelength. The wavelength cutoff by the quartz reactor was <190 nm. External anodic bias was applied by a DC potentiostat (RXN-305D, Shenzhen Zhaoxin Power Co. Ltd, China). After a defined irradiation period, 3.0 mL of dispersion was centrifuged and the supernatant was analyzed for the rhodamine B concentration. The measurements were completed by monitoring its absorption at a wavelength of 554 nm using a UV-Vis spectrophotometer (Agilent Cary 300 UV-Vis, Agilent, USA). The removal efficiency (%) was calculated using the following equation:

$$Removal\ efficiency\ (\%) = \frac{C_0 - C_t}{C_0} \times 100$$

where C_0 and C_t (mg/L) are the initial concentration of rhodamine B and its concentration at time t in the solution, respectively. For comparisons, a photocatalytic process and an electrocatalytic process were also tested by removing the cell voltage and light irradiation, respectively.

RESULTS AND DISCUSSION

### Characterization of the composite

SEM results

The specific surface area of the $ZnFe_2O_4/TiO_2$/flake graphite composite was determined by a N_2 physisorption isotherm method. The composite has a BET specific surface area of 2.7470 m^2/g, which is higher than that of bare flake graphite, 1.7605 m^2/g. The surface morphology of the composite and flake graphite measured by SEM is shown in Figure 2. The bare flake graphite is illustrated in Figure 2(a). Prior to any modification, the surface appeared smooth, without any obvious impurities. After aggregation with metal oxides and calcinations, the surface became rough and dispersed with particles (Figure 2(b)). This was in close agreement with the observation of increased specific surface area. The particles on the surface were produced by the aggregation of $ZnFe_2O_4$ and TiO_2, and neither possess any definite shape. The increased specific surface area could benefit the heterogeneous photocatalysis by facilitating surface adsorption of reactants and thus promoting the interfacial charge transfer (Lee *et al.* 2013).

XRD results

In order to examine the crystal phases of the prepared composite, qualitative analysis of the XRD pattern was performed. Figure 2(c) compares the XRD patterns for the composite and bare flake graphite. The peak of anatase TiO_2 phase was observed at 2θ = 25.281° while the peak of $ZnFe_2O_4$ was not found in the XRD pattern of the composite. The non-existence of the aggregate was attributed to low content or high dispersion of the species within the composite (Xu *et al.* 2011). Meanwhile, the intensity of the XRD peak is also dictated by the degree of crystallization, which is influenced by the calcination temperature, and Lee *et al.* (2013) found that increasing the calcination temperature from 450 to 750 °C would lead to a higher peak formation. It is noted that the XRD pattern of the composite sample with optimum PEC performance was presented. Increasing the weight percentages of $ZnFe_2O_4$ visualized the peak, but was found to have lower PEC performance.

XPS results

The chemical state of each element in the $ZnFe_2O_4/TiO_2$/flake graphite composite was studied by XPS analysis. The
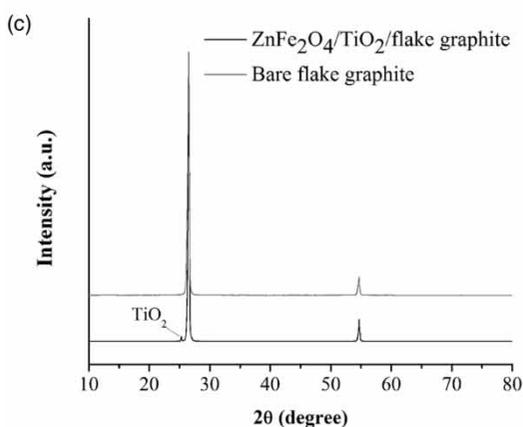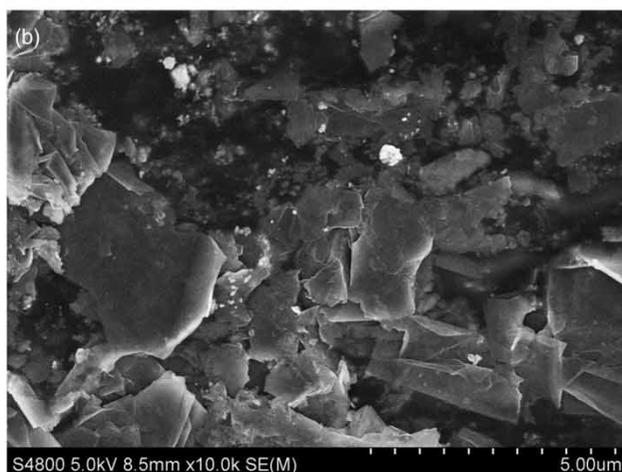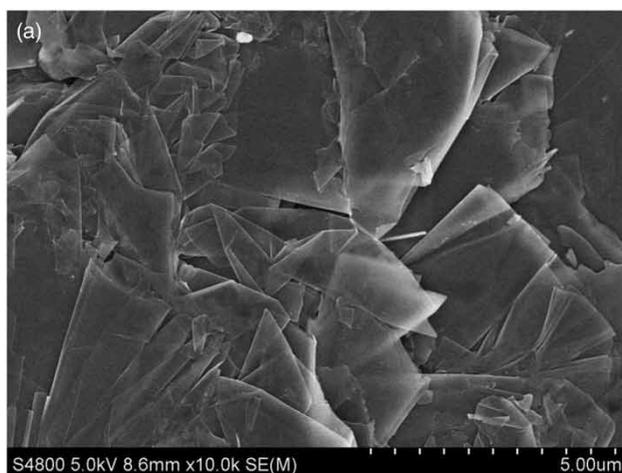
Figure 2 | Imaging and surface analysis of $ZnFe_2O_4/TiO_2$/flake graphite composite: (a) SEM image of bare flake graphite; (b) SEM image of $ZnFe_2O_4/TiO_2$/flake graphite composite; and (c) XRD patterns.

XPS survey spectrum of the composite is illustrated in Figure 3(a) and the core level spectra of characteristic elements are presented in Figure 3(b)–3(e). The survey spectrum confirms that besides the C element in flake graphite, Fe, Ti, Zn, and O were also present in the composite material. The results were in accordance with the explanation of XRD results on the disappearance of $ZnFe_2O_4$ peak due to low content and high dispersion of the aggregate. High resolution XPS spectrum of Ti 2p was observed in Figure 3(b). The peaks in the Ti 2p spectra located at the binding energy of 464.4 eV and 458.6 eV were indicative of Ti $2p_{1/2}$ and Ti $2p_{3/2}$ of Ti^{4+}, respectively (Joung *et al.* 2006). As shown in Figure 3(c), the binding energy of 710.6 eV and 724.4 eV were ascribed to the Fe $2p_{1/2}$ and Fe $2p_{3/2}$ of the oxidation state Fe^{3+}, respectively. The peaks in the Zn 2p spectra, as shown in Figure 4(d), were indicative of Zn $2p_{1/2}$ and Zn $2p_{3/2}$ of Zn^{2+} (NuLi *et al.* 2004), located at the binding energy of 1,045.02 eV and 1,021.79 eV, respectively. The peak at 529.93 eV (Figure 3(e)) was due to O 1 s bonded to Ti and Fe, whereas the peak at higher binding energy of 531.82 eV was ascribed to the presence of the OH group (Palanisamy *et al.* 2013), indicating surface contamination by hydroxides from the atmosphere.

On the basis of the SEM images, XRD patterns, and XPS spectra, it is reasonable to suggest that the heterojunctions of the composite were present in the as-synthesized sample.

Operating conditions

PEC process

The influence of different processes including direct photocatalysis, electrocatalysis, and PEC degradation of rhodamine B were studied. Compared to the operating conditions of the PEC process, direct photocatalysis and electrocatalysis did not include cell voltage and light irradiation, respectively. The reactions for all three processes were carried out for 90 min and the progress of each reaction was monitored by UV absorbance measurement at a time interval of 10 min to examine the degradation performance.

The results indicate that rhodamine B could be removed from the solution by all three processes, and the profiles are presented in Figure 4. However, only 22.1% of rhodamine B was removed by direct photocatalysis within 90 min, compared to 63.2% removal by the electrocatalysis when a bias potential was applied. These two removal efficiencies were both apparently lower than that of the PEC process (96.2%). The increased removal efficiency for the PEC process implied an obvious synergistic effect between the electrocatalysis and photocatalysis, suggesting that the applied bias potential inhibited the recombination of
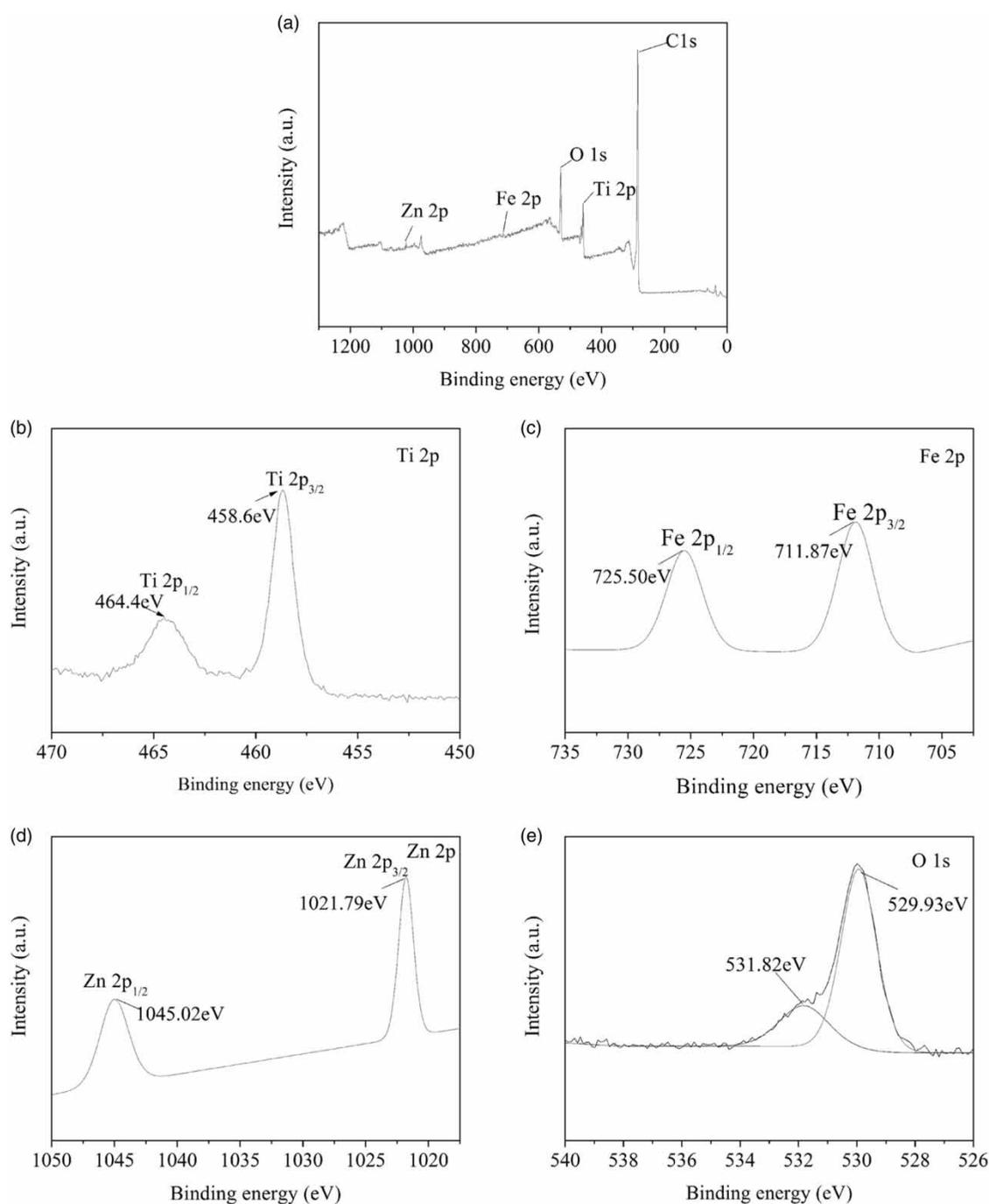
Figure 3 │ XPS spectra of ZnFe2O4/TiO2/flake graphite composite: (a) survey spectrum; (b) Ti 2p spectrum; (c) Fe 2p spectrum; (d) Zn 2p spectrum; and (e) O 1 s spectrum.

photoinduced electron-hole pairs effectively and prolonged the lift of the photoinduced carriers (Hou *et al.* 2010). The external electric field could also result in direct (direct electron transfer on the anode) or indirect (electro-generated oxidizing species, i.e. •OH, from water electrolysis) electrochemical oxidation of organics. Besides, the carbonaceous material in flake graphite might serve as a catalyst to

decompose H_2O_2 to •OH due to the presence of polyaromatic moieties and functional group (Can *et al.* 2014), leading to higher concentration of •OH. Moreover, the use of the composite as particle electrodes resulted in expanded specific surface areas contributing to a greater collecting capacity of photoinduced electrons than those with holes (An *et al.* 2004), and could form numerous charged
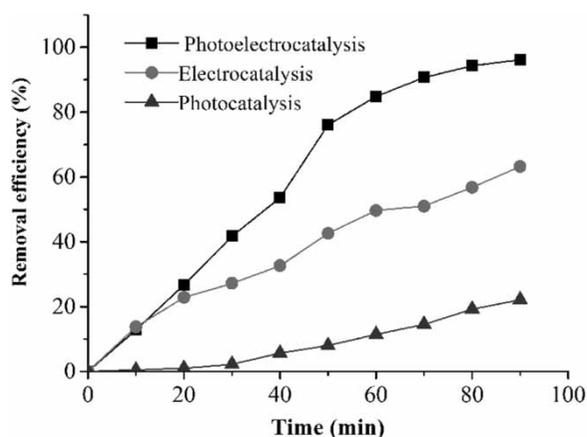
Figure 4 │ Effect of photocatalytic, electrocatalytic, and photoelectrocatalytic processes on the removal efficiency of rhodamine B using $ZnFe_2O_4/TiO_2$/flake graphite composite as particle electrodes (operating conditions are $[Na_2SO_4]$ = 0.010 mol/L, applied cell voltage = 12 V, air flow = 20 mL/min, composite dosage = 8 g/L, solution pH = 7.3, and [rhodamine B] = 10 mg/L).

microelectrodes shortening the distance between the reactants and the electrodes (Kong *et al.* 2006). Thus, the surface area of the electrodes and the mass transfer rates were increased, resulting in higher degradation efficiency. The above discussion explains the phenomenon of the enhanced rhodamine B removal by the PEC process. The life of the composite was also investigated by repeated uses of the composite, and the removal efficiency of PEC degradation decreased by 10% after five cycles of operation.

Electrolyte concentration

Adding electrolyte to a reaction solution can enhance the conductivity and increase the electron mass transfer. Na_2SO_4 is used as a supporting electrolyte, because it can offer excess levels of sulfate anions, which can enhance the charge transfer. It may also be oxidized to peroxydisulfate anions or an even stronger oxidant sulfate radical anions (Zhang *et al.* 2012). The influence of Na_2SO_4 on the PEC degradation of rhodamine B with the novel composite has been investigated in 0.005, 0.010, 0.020, and 0.030 mol/L concentrations. As shown in Figure 5(a), the rhodamine B removal efficiency increased as the Na_2SO_4 concentration increased from 0.005 to 0.010 mol/L. This was because the electricity current increased in the system and more excited electrons under light irradiation were transferred from the anode to the cathode, which resulted in lower recombination of the electron-hole pairs. There was no significant change in the removal efficiency when the Na_2SO_4 concentration increased further. This was attributed to the more parasitic reactions, i.e. the deposition of

H_2O_2, as a result of higher current level. Thus, it would be more economical to use 0.010 mol/L Na_2SO_4 on an industrial scale.
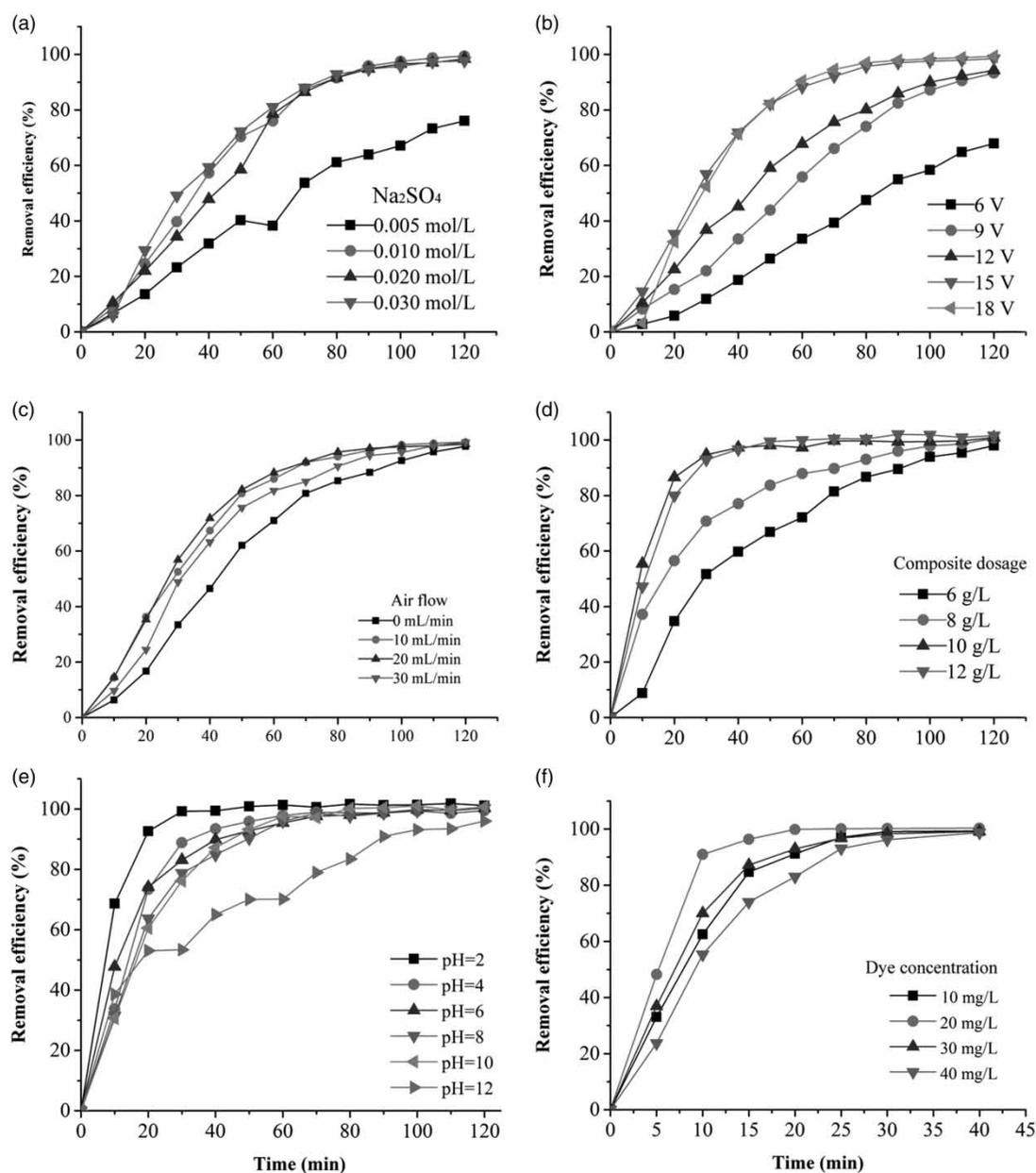
Applied cell voltage

Applying a potential bias to electrodes using a potentiostat can minimize the recombination of photoinduced electron-hole pairs (Wang *et al.* 2012; Zhai *et al.* 2013). The cell voltage is also the driving force in the electrocatalytic reaction and plays an important factor in wastewater treatment involving the electrochemical method. The influence of an applied cell voltage on the PEC degradation of rhodamine B with the novel composite is shown in Figure 5(b). The removal efficiency increased with an increasing potential bias, up to 15 V. This phenomenon could be attributed to an increase in the electrostatic interaction and affinity between the surface of the electrode and ions due to increased adsorption at high potentials (Ayoubi-Feiz *et al.* 2014). The capability for direct or indirect electrochemical oxidation of the dye pollutant was enhanced. Furthermore, by increasing the electric field, the separation of photoinduced electron-hole pairs inside the semiconductors was enhanced, which might result in the enhancement of •OH generation (Jiang *et al.* 2004).

It should also be noted that when the applied cell voltage increased higher than 15 V, the removal efficiency did not further increase. This was because higher potential not only led to more parasitic reactions such as the decomposition of H_2O_2 and significant simultaneous H_2 generation, but also caused higher energy consumption (Liu *et al.* 2012). The corrosion of electrodes and higher solution temperature might also lead to the leaching of adsorbed pollutants.

Air flow

The PEC degradation of rhodamine B with the novel composite was compared under no aeration and aeration with air flow of 10, 20 and 30 ml/min. The observed rhodamine B removal percentages are shown in Figure 5(c). With aeration, the removal efficiency of rhodamine B increased. This was because aeration agitated the solution and offered better gas-liquid mass transfer efficiency. On the other hand, the molecular oxygen played an important role in the photocatalytic reaction by supplying essential oxygen to capture photoinduced electrons, reducing the recombination of photoinduced electron-hole pairs (An *et al.* 2004).

It is noted that the improvement in removal efficiency was not observed when the air flow further increased from 20 to 30 mL/min. This implied that necessary aeration was

Figure 5 │ Effects of operating conditions on the PEC degradation of rhodamine B with $ZnFe_2O_4/TiO_2$/flake graphite composite as particle electrodes: (a) electrolyte concentration; (b) applied cell voltage; (c) air flow; (d) composite dosage; (e) solution pH; and (f) dye concentration. (Unless noted on each figure, operating conditions held constant are $[Na_2SO_4] =$ 0.010 mol/L, applied cell voltage = 15 V, air flow = 20 mL/min, composite dosage = 10 g/L, solution pH = 7.3, and [rhodamine B] = 10 mg/L.)

beneficial but a large air flow was not favorable. The phenomenon could be attributed to the saturation of dissolved oxygen and the reduced adsorption of the pollutant onto the composite surface caused by a large air flow.

Composite dosage

The amount of catalyst in the PEC process is significant as it may strongly influence the degradation effect. The PEC

experiments were carried out by varying the composite dosage from 6 to 12 g/L. As shown in Figure 5(d), the removal efficiency of rhodamine B increased when the amount of composite increased from 6 to 10 g/L, attributable to a pronounced increase in the active sites available on the composite surface. An optimum composite dosage also offered a reasonable light absorption to produce sufficient amounts of active •OH on the surface of the composite. A further increase in the dosage beyond 10 g/L

showed a decrease in degradation performance. This was ascribed to the decrease of total active surface area by flake graphite overlapping, deactivation of activated molecules by collision with ground state molecules (Zhou *et al.* 2005), and agglomeration (Wu *et al.* 2009).

Solution pH

To study the effect of pH on the PEC degradation of rhodamine B with the novel composite, experiments were carried out in a pH range of 2–12. As shown in Figure 5(e), removal efficiency for rhodamine B increased as pH value decreased. It is known that the pH level may affect discolorization and mineralization of dyes differently (Zhang *et al.* 2012). In this study, the optimum pH value for the PEC degradation of rhodamine B was found to be 2. Since the point of zero charge (pH_{pzc}) for TiO_2 is around 6 (Selcuk & Bekbolet 2008), the catalyst surface is negatively charged when the pH is higher than the pH_{pzc} or positively charged when the pH is lower. It is speculated that the solution pH affects the sorption of dyes on the catalyst surface, which depends on the dye functional group. Rhodamine B has a pKa of 3.0 and was negatively charged with only one ionized carboxylic group (Kasnavia *et al.* 1999) while the catalyst was positively charged at pH 2, the adsorption of rhodamine B onto the catalyst surface became much easier. Beltrán *et al.* (1996) also reported a disadvantageous effect existed with an increased solution pH due to a stronger scavenging effect until the pH value was higher than the pKa of hydrogen peroxide (11.8). This explained why a low pH was preferred for rhodamine B removal with the system.

Dye concentration

To explore the maximum PEC degradation capacity with the novel composite, the effect of dye concentration on degradation performance was investigated at rhodamine B concentrations of 10, 20, 30, and 40 mg/L as a function of irradiation time at optimum conditions ($Na_2SO_4 = 0.01$ mole/L, applied cell voltage = 15 V, air flow = 20 mL/min, composite dosage = 10 g/L, and solution pH = 2). As shown in Figure 5(f), higher removal efficiencies were observed by starting with higher rhodamine B concentrations up to 20 mg/L. Increasing concentrations higher than 20 mg/L led to lower removal efficiencies. This was because the number of active sites on the composite adsorbent was not enough for all of the dye molecules in a high dye concentration (Wang *et al.* 2013). Furthermore, high concentration dyes absorbed part of the light, or the low transparency

Table 1 | Pseudo-first-order rate constant values and regression coefficients of PEC process with ZnFe₂O₄/TiO₂/flake graphite composite as particle electrodes at various rhodamine B concentrations (operating conditions are $[Na_2SO_4]$ = 0.010 mol/L, applied cell voltage = 15 V, air flow = 20 mL/min, composite dosage = 10 g/L, and solution pH = 2)

Rhodamine B concentration	10 mg/L	20 mg/L	30 mg/L	40 mg/L
Pseudo-first-order rate constant k (min^{-1})	0.139	0.278	0.126	0.113
Regression coefficient R^2	0.960	0.942	0.979	0.988

reduced the light intensity reaching the composite surface, leading to a reduction of efficiency due to decline in the amount of ·OH generation (Cardoso *et al.* 2010).

It was found that a 99.0% removal efficiency was achievable within 30 min of PEC treatment under optimum conditions of 0.01 mol/L Na_2SO_4, applied cell voltage of 15 V, air flow of 20 mL/min, composite dosage of 10 g/L, solution pH of 2, and rhodamine B concentration of 20 mg/L. Table 1 presents the pseudo-first-order rate constants and regression coefficients for PEC degradation with the novel composite at rhodamine B concentrations of 10, 20, 30, and 40 mg/L while all other conditions were optimum. The results indicated that the degradation followed pseudo-first-order kinetics with high regression coefficients. The rate constant increased as the dye concentration increased from 10 to 20 mg/L and then decreased. The degradation rate constant at 10 mg/L was relatively low, because the process was dictated by the absorption rate of dye to the active sites of the composite, and a lower concentration led to a less favorable concentration gradient for diffusion of the dye onto the composite. On the other hand, the number of ·OH formed as a result of the PEC process under certain light and voltage scenario was fixed or even decreased as the dye concentration increased further, and the reaction between ·OH and dye became rate-limiting. At the optimum conditions, the pseudo-first-order rate constant was 0.278 min^{-1}.

Implications

Rhodamine B – one of the most commonly used dyes in the textile and food industry, is highly carcinogenic, a neurotoxin and chronic as a pollutant in drinking water. In this study, dye concentrations up to 40 mg/L (0.084 mM) were explored to simulate wastewater contaminated with a high level of Rhodamine B. Thus, it must be treated carefully before being discharged into water streams. Although many researchers have confirmed that two-dimensional systems are able to get the treatment job done, with a

three-dimensional electrode system, the electrochemical process shows a better process as a result of the formation of numerous micro-electrodes in the electrical field. Moreover, the heterogeneous photocatalysis appears to be a promising route combined with the three-dimensional system for the treatment of the dye as demonstrated by the high degradation efficiency in this study, and it overcomes previous major drawbacks such as inefficient light harvesting, design of photo reactor, and the recovery and reuse of titanium dioxide. The study presents a promising result which should provide motivation to build a larger scale PEC system and eventually to make commercial PEC systems a reality.

CONCLUSION

The $ZnFe_2O_4/TiO_2$/flake graphite composite has been synthesized and characterized by SEM, XRD and XPS techniques. The results revealed that the composite is a good catalyst as particle electrodes for the PEC degradation of rhodamine B due to a synergistic effect of photocatalysis and electrocatalysis. The PEC degradation performance was dependent on electrolyte concentration, applied cell voltage, air flow, composite dosage, solution pH, and dye concentration. A 99.0% rhodamine B removal efficiency was observed within 30 min of PEC treatment under optimum conditions of 0.01 mol/L Na_2SO_4, applied cell voltage of 15 V, air flow of 20 mL/min, composite dosage of 10 g/L, solution pH of 2, and rhodamine B concentration of 20 mg/L. The $ZnFe_2O_4/TiO_2$/flake graphite composite as particle electrodes is expected to have promising applications for the degradation of residual dyes in water.

ACKNOWLEDGEMENTS

REFERENCES

An, T. C., Zhu, X. H. & Xiong, Y. 2002 Feasibility study of photoelectrochemical degradation of methylene blue with three-dimensional electrode-photocatalytic reactor. *Chemosphere* **46**, 897–903.

An, T., Zhang, W., Xiao, X., Sheng, G., Fu, J. & Zhu, X. 2004 Photoelectrocatalytic degradation of quinoline with a novel three-dimensional electrode-packed bed photocatalytic reactor. *Journal of Photochemistry and Photobiology A: Chemistry* **161**, 233–242.

Ayoubi-Feiz, B., Aber, S., Khataee, A. & Alipour, E. 2014 Preparation and application of α-Fe_2O_3/TiO_2/activated charcoal plate nanocomposite as an electrode for electrosorption-assisted visible light photoelectrocatalytic process. *Journal of Molecular Catalysis A: Chemical* **395**, 440–448.

Beltrán, F. J., Ovejero, G. & Rivas, J. 1996 Oxidation of polynuclear aromatic hydrocarbons in water. 3. UV radiation combined with hydrogen peroxide. *Industrial & Engineering Chemistry Research* **35**, 883–890.

Can, W., Yao-Kun, H., Qing, Z. & Min, J. 2014 Treatment of secondary effluent using a three-dimensional electrode system: COD removal, biotoxicity assessment, and disinfection effects. *Chemical Engineering Journal* **243**, 1–6.

Cardoso, J. C., Lizier, T. M. & Zanoni, M. V. B. 2010 Highly ordered TiO_2 nanotube arrays and photoelectrocatalytic oxidation of aromatic amine. *Applied Catalysis B: Environmental* **99**, 96–102.

Hou, Y., Li, X. Y., Zhao, Q. D., Quan, X. & Chen, G. H. 2010 Electrochemical method for synthesis of a $ZnFe_2O_4/TiO_2$ composite nanotube array modified electrode with enhanced photoelectrochemical activity. *Advanced Functional Materials* **20**, 2165–2174.

Jiang, Z., Wang, H., Huang, H. & Cao, C. 2004 Photocatalysis enhancement by electric field: TiO_2 thin film for degradation of dye X-3B. *Chemosphere* **56**, 503–508.

Joung, S. K., Amemiya, T., Murabayashi, M. & Itoh, K. 2006 Relation between photocatalytic activity and preparation conditions for nitrogen-doped visible light-driven TiO_2 photocatalysts. *Applied Catalysis A: General* **312**, 20–26.

Kasnavia, T., Vu, D. & Sabatini, D. A. 1999 Fluorescent dye and media properties affecting sorption and tracer selection. *Ground Water* **37**, 376–381.

Kong, W. P., Wang, B., Ma, H. Z. & Gu, L. 2006 Electrochemical treatment of anionic surfactants in synthetic wastewater with three-dimensional electrodes. *Journal of Hazardous Materials* **137**, 1532–1537.

Lee, S. S., Bai, H., Liu, Z. & Sun, D. D. 2013 Novel-structured electrospun TiO_2/CuO composite nanofibers for high efficient photocatalytic cogeneration of clean water and energy from dye wastewater. *Water Research* **47**, 4059–4073.

Liu, W., Ai, Z. & Zhang, L. 2012 Design of a neutral three-dimensional electro-Fenton system with foam nickel as particle electrodes for wastewater treatment. *Journal of Hazardous Materials* **243**, 257–264.

Mourão, H. A. J. L., Malagutti, A. R. & Ribeiro, C. 2010 Synthesis of TiO_2-coated $CoFe_2O_4$ photocatalysts applied to the

photodegradation of atrazine and rhodamine B in water. *Applied Catalysis A: General* **382**, 284–292.

NuLi, Y.-N., Chu, Y.-Q. & Qin, Q.-Z. 2004 Nanocrystalline $ZnFe_2O_4$ and Ag-doped $ZnFe_2O_4$ films used as new anode materials for Li-ion batteries. *Journal of the Electrochemical Society* **151**, A1077–A1083.

Palanisamy, B., Babu, C. M., Sundaravel, B., Anandan, S. & Murugesan, V. 2013 Sol-gel synthesis of mesoporous mixed Fe_2O_3/TiO_2 photocatalyst: application for degradation of 4-chlorophenol. *Journal of Hazardous Materials* **252–253**, 233–242.

Pan, J. H., Dou, H., Xiong, Z., Xu, C., Ma, J. & Zhao, X. S. 2010 Porous photocatalysts for advanced water purifications. *Journal of Materials Chemistry* **20**, 4512–4528.

Selcuk, H. & Bekbolet, M. 2008 Photocatalytic and photoelectrocatalytic humic acid removal and selectivity of TiO_2 coated photoanode. *Chemosphere* **73**, 854–858.

Wang, D., Li, X., Chen, J. & Tao, X. 2012 Enhanced photoelectrocatalytic activity of reduced graphene oxide/TiO_2 composite films for dye degradation. *Chemical Engineering Journal* **198**, 547–550.

Wang, Y., Zhang, Y. N., Zhao, G., Wu, M., Li, M., Li, D., Zhang, Y. & Zhang, Y. 2013 Electrosorptive photocatalytic degradation of highly concentrated *p*-nitroaniline with TiO_2 nanorod-clusters/carbon aerogel electrode under visible light. *Separation and Purification Technology* **104**, 229–237.

Wu, Y., Zhang, J., Xiao, L. & Chen, F. 2009 Preparation and characterization of TiO_2 photocatalysts by Fe^{3+} doping together with Au deposition for the degradation of organic pollutants. *Applied Catalysis B: Environmental* **88**, 525–532.

Xu, S., Ng, J., Du, A. J., Liu, J. & Sun, D. D. 2011 Highly efficient TiO_2 nanotube photocatalyst for simultaneous hydrogen production and copper removal from water. *International Journal of Hydrogen Energy* **36**, 6538–6545.

Zhai, C., Zhu, M., Ren, F., Yao, Z., Du, Y. & Yang, P. 2013 Enhanced photoelectrocatalytic performance of titanium dioxide/carbon cloth based photoelectrodes by graphene modification under visible-light irradiation. *Journal of Hazardous Materials* **263**, 291–298.

Zhang, Y., Xiong, X., Han, Y., Zhang, X., Shen, F., Deng, S., Xiao, H., Yang, X., Yang, G. & Peng, H. 2012 Photoelectrocatalytic degradation of recalcitrant organic pollutants using TiO_2 film electrodes: an overview. *Chemosphere* **88**, 145–154.

Zhou, M., Yu, J. & Cheng, B. 2005 Preparation and photocatalytic activity of Fe-doped mesoporous titanium dioxide nanocrystalline photocatalysts. *Materials Chemistry and Physics* **93**, 159–163.